



Facile one-pot solvothermal synthesis of magnetic mesoporous carbon for the efficient adsorption of methyl orange

Ruonan Chen¹ · Shiman Zhai¹ · Weihua Lu¹ · Jinwei Wei¹ · Jiangyan Xu¹ · Aimin Lu¹ · Hongmei Jiang¹ 

Received: 27 August 2019 / Accepted: 22 December 2019 / Published online: 3 January 2020
© Springer-Verlag GmbH Germany, part of Springer Nature 2020

Abstract

A facile one-pot solvent thermal method was proposed to synthesize magnetic mesoporous carbon (MMC) using $\text{Fe}(\text{NO}_3)_3 \cdot 9\text{H}_2\text{O}$ as a precursor, Pluronic copolymer P123 as template, and chitosan as carbon source, and it was applied for the adsorptive remediation of methyl orange (MO). The characterization results of TEM, XRD, and IR showed that MMC consisted of graphitized carbon matrix and some black spherical particle mixture of Fe_3O_4 and Fe, and it was rich in hydroxyl and carbonyl groups. Besides, the effect of the content of Fe and the content of chitosan in MMC on the magnetism and adsorption performance of prepared material were investigated. In addition, the effects of pH value, initial concentration of methyl orange, and contact time on the adsorption performance of MO were studied, respectively. At 318 K, the maximum adsorption capacity of MO calculated from Langmuir isotherm was from 139 to 400 mg g^{-1} on MMC. Kinetic studies demonstrated that the adsorption process obeyed a pseudo-second-order kinetic model. The regeneration experiments revealed that MMC could be reused at least five times without notable decrease of adsorption performance. These results illustrate that MMC is an efficient and economical adsorbent for the adsorption of MO.

Keywords One-pot solvent thermal method · Magnetic mesoporous carbon · Methyl orange · Adsorption

Introduction

The design, fabrication, and modification of mesoporous carbon materials (MC) have drawn much attention because they have demonstrated excellent performances in various application fields such as catalyst supports (Ghughe and Saroha 2018; Zhang et al. 2015), energy storage and conversion systems (Wang et al. 2018; Su et al. 2012; Li et al. 2015), electrochemical sensors (Walcarius 2017), and adsorbents (Hao et al. 2010; Libbrecht et al. 2017; Tripathi et al. 2014) due to their fascinating features, for example, large specific surface area, porous structure and tunable pore size, and good chemical and thermal stability (Suib 2017). The controllability of mesopore size and a variety of their pore structures can make MC serve as very attractive and effective adsorbents. Moreover, MC can interact with analytes not only on their surface but also

throughout the bulk of the materials, which contributes to high adsorption performance.

It is more attracting to explore the possibility of improving or extending their properties by introducing functional nanoparticles in MC matrix (Zhang et al. 2016). Various nanoparticles have been introduced into MC, such as sulfide (Liu et al. 2019), metal oxides (Coromelci-Pastravanu et al. 2014; Fuertes et al. 2007; Liu et al. 2014), and metals (Holec et al. 2018). In particular, magnetic nanoparticles are of great scientific interest for catalysis and adsorption because the deposited magnetic nanoparticles can provide a high strong magnetic response (Ma et al. 2017; Liang et al. 2016), which can offer easily separating and recovering adsorbents from the reaction medium by an outer magnet and reducing the energy consumption. Besides, the combination of magnetic nanoparticles and MC (magnetic mesoporous carbon (MMC)) can improve the stability of magnetic nanoparticles by confinement inside the carbon matrix, thus avoiding the oxidation or dissolving of nanoparticles during the application. In addition, the restriction on magnetic nanoparticles by carbon matrix can control the growth of the particles, providing tunable particle size.

Generally, the surface area and pore structure, depending on the synthesis approaches, are two key factors affecting the

Responsible editor: Tito Roberto Cadaval Jr

✉ Hongmei Jiang
jianghongmei@njau.edu.cn

¹ College of Science, Nanjing Agricultural University, Weigang Street 1#, Nanjing 210095, China

adsorption performance of the adsorbents, so far, a large number of synthetic strategies have been reported for the fabrication of MMC, in which post-loading or nanocasting method were commonly adopted according to the review of Zhao (Deng et al. 2011). When using post-loading method, magnetic nanoparticles were loaded into the pre-synthesized MC or an inorganic precursor was impregnated into the pores of MC (Deng et al. 2017; Li et al. 2017a; b; Yadaei et al. 2018; Wu et al. 2012) followed by in situ conversion of the precursor into magnetic nanoparticles through thermal treatment. Although post-loading approach can retain the morphology and size uniformity of MC, it requires multiple complicated synthetic steps. More importantly is the introduction of magnetic nanoparticles in porous hosts can block the main pores of mesoporous materials, leading to low pore volume, low surface area, and poor accessibility of pores. In order to solve these problems, another nanocasting method (Zeng et al. 2015; Liu et al. 2016; Tang et al. 2014; Dai et al. 2018) is proposed, in which the precursors of carbon and metal are impregnated into the mesopore channels of hard templates and then carbonized by thermal treatment and removed hard templates through dissolving or calcining at last. Usually, it is not easy to avoid the etching of magnetic nanoparticles prepared by nanocasting method in acidic solution, which will result in losing their magnetism and hard separating by an outer magnet.

The principle of the foregoing two techniques is easy to understand, and the prepared material by these methods can provide high surface area and offer large adsorption capacity, which makes them achieve intensive application for the adsorption of Cd(II) (Quiroa-Montalván et al. 2017; Li et al. 2017a; b; Zeng et al. 2015), Cr(VI) (Li et al. 2017a; b; Tang et al. 2014), As(III) (Wu et al. 2012), As(V) (Wu et al. 2012), Pb(II) (Quiroa-Montalván et al. 2017), Hg(II) (Liu et al. 2016), and dye (Deng et al. 2017; Dai et al. 2018). Normally, the fabricating progress of post-loading, needing several steps, is a little tedious and complex. As for nanocasting, it needs to sacrifice hard template, causing serious wasting. In order to improve the efficiency of the MMC as adsorbents, a facile one-pot strategy is proposed, which involves mixing and carbonating of the precursors of metal and carbon using porogen as template or combining with the self-assembly of amphiphilic block copolymers, allowing the simultaneous formation of the mesoporous carbonaceous matrix with in situ generating magnetic nanoparticles with no need of reducing treatment. Wu's group (Li et al. 2017a; b) has proposed a new kind of magnetic mesoporous carbon prepared by the one-step carbonization of a hybrid precursor of glucose, melamine, and iron chloride using KCl/ZnCl₂ as the porogen. Gao's group (Ma et al. 2017) has synthesized a magnetic mesoporous carbon through a simple one-pot route using the biomass chitosan and Fe(NO₃)₃ as precursors and NaCl as template agent. The materials prepared by the above

methods both displayed an effective adsorption behavior. Zhao's group (Zhai et al. 2009) has reported a facile and convenient method to prepare MMC using Resol and ferric citrate as the precursors and triblock copolymer F127 as a template via a solvent evaporation-induced self-assembly method. Furthermore, in order to improve the adsorption and magnetic performance of the materials, the effect of the amount of metal precursor on pore features and magnetic properties was intensively examined by Zhao's group.

Chitosan, known as harmless biopolymers, is abundant in amino and hydroxyl functional groups, which makes it a high adsorption potential for various pollutants in the water treatment (Yadaei et al. 2018). Taking into account the foregoing viewpoints, we report a convenient one-pot solvent thermal method to fabricate magnetic mesoporous carbon using Fe(NO₃)₃·9H₂O as a metal precursor, chitosan as carbon source, and Pluronic copolymer P123 as template. Compared with the study of Zhao's group, solvent thermal procedure can save evaporation time. Besides, in order to make sure the relationship between the structure and performance, the effect of the amount of carbon precursors and the amount of metal precursor on the adsorption performance and magnetism of MMC will be investigated in detail. To study the adsorption performance of the prepared MMC, methyl orange (MO) is selected as analyte. The effects of pH value, initial concentration of methyl orange, contact time, and temperature on the adsorption quantity of methyl orange will be evaluated, respectively.

Experimental

Materials and standard solution

All the reagents and chemicals used in this study were of analytical grade without further purification. The medium viscosity chitosan (CS) was purchased from Shanghai Ryon Biological Technology Co., Ltd. (Shanghai, China). Ferric nitrate nonahydrate (Fe(NO₃)₃·9H₂O) and acetic acid solution 36% were ordered from Sinopharm Chemical Reagent Co., Ltd. (Shanghai, China). Polyethylene oxide–polypropylene oxide–polyethylene oxide (P123) and tetraethyl orthosilicate (TEOS) were provided by Aldrich (Shanghai, China). MO standard solution (1 g L⁻¹) used in this experiment was prepared by dissolving 1 g MO powder with 1 L ultrapure water.

Preparation of magnetic mesoporous carbon composite

Magnetic mesoporous carbon composite was synthesized by one-pot solvent thermal route based on the modified approach reported by Zhao's group (Zhai et al. 2009). The detailed experiment parameters, adsorption performance, and

magnetism of the products prepared in this work are shown in Table 1. In brief, 1 g of P123 and a certain amount of $\text{Fe}(\text{NO}_3)_3 \cdot 9\text{H}_2\text{O}$ (0.606, 0.808, and 1.212 g) were mixed into 10 mL of ethanol solution with stirring violently at room temperature until clarification. Meanwhile, a given amount of CS (0.1, 0.25, and 0.5 g) was added into the mixture of 40 mL of ethanol and acetic acid with a volume ratio of 1:1 respectively and stirred at 30 °C for 2 h and then transferred into the solution made in first step at the speed of 1 day s^{-1} using a peristaltic pump. After stirring for another 30 min, 3 mL of TEOS was dropped into the reaction solution with the speed of 3 days s^{-1} and stirred for 3 h to give it a full reaction. Afterwards, the mixture was poured into a 100 mL of stainless steel autoclave with Teflon lining and heated in an oven at 110 °C for 24 h. The obtained brown gel was dried in an oven at 60 °C for 12 h and then calcinated (700 and 900 °C) under the atmosphere of nitrogen. Finally, the composite was washed three times with sodium hydroxide solution and deionized water, respectively, and then dried at 60 °C.

Characterization

The microstructure of MMC was observed by S-3400N II transmission electron microscope (TEM) (Hitachi, Tokyo, Japan). V-Sorb 2800P-specific surface area analyzer (BET) (Gold APP Instrument, Beijing, China) was utilized to detect the specific surface area and aperture of the sample by N_2 adsorption/desorption. The FT-IR spectra were recorded by Fourier transform infrared spectrometer (Thermo Nicolet, USA) within a range of 400–4000 cm^{-1} . Powder X-ray diffraction (XRD) data were acquired using an X'TRA X-ray diffractometer (ARL, Switzerland). CyberScan pH 2100 pH meter (Eutech, USA) was used to measure the pH values. All reactions in the experiment were carried out in a KH-500 ultrasonic bath (Kunshan Hechuang Ultrasonic Instrument, Suzhou, China) to enhance the adsorption efficiency.

Adsorption experiments

All adsorption experiments in this study were conducted in a batch mode, and all reactions were carried out in an ultrasonic bath. The effect of pH on the adsorption capacity was measured by adding 2 mg adsorbent into 40-mL 110 mg L^{-1} MO

solution with pH varying from 2 to 7. Then, the beakers with mixed solution were soaked in the ultrasonic bath for 30 min to speed up the adsorption equilibrium. The adsorbent was separated using a magnetic field, and the supernatant solution was collected to acquire the residual concentration by using UV-Vis spectrophotometer at a wavelength of 470 nm.

Isotherm experiments were carried out by changing the initial MO concentrations ranging from 10 to 110 mg L^{-1} by adding 2 mg adsorbent into 40 mL reaction mixture under the condition of pH = 4. The same experiment was conducted at 25, 35, and 45 °C, respectively. The other procedure was the same as the experiments for pH effect.

Kinetic experiments were studied by varying the contact time from 5 to 80 min. The other procedure was the same as the isotherm experiments.

The removal rate ($R\%$) and adsorption capacity (Q) of MO were calculated using the following formula:

$$R\% = (C_0 - C_e) / C_0 \times 100\% \quad (1)$$

$$Q = (C_0 - C_e) \times V / m \quad (2)$$

where C_0 and C_e are the initial concentration of MO (mg L^{-1}) before adsorption and the equilibrium concentration of MO (mg L^{-1}) after adsorption, m is the mass of the adsorbent (mg), V is the volume of MO solution (mL), and Q is the adsorption capacity (mg g^{-1}).

Regression analysis

Nonlinear regression was adopted to fit the equilibrium data and kinetic data. The parameters were determined through Quasi-Newton estimation method by use of the Origin software. The fits quality of the model was evaluated by coefficient of the determination (R^2) and average relative error (ARE) (Cadaval et al. 2015; Rodrigues et al. 2018).

The feasibility of desorption and regeneration of the adsorbent was evaluated using 0.1 mol L^{-1} NaOH. Typically, 40 mL desorbing agents with 2 mg MO-loaded MMC were ultrasonically treated for 60 min and then were magnetically separated. The adsorbent was washed with deionized water for three times and then directly used for the next cycle. Five sequential cycles of adsorption–desorption were carried out.

Results and discussion

Characterization

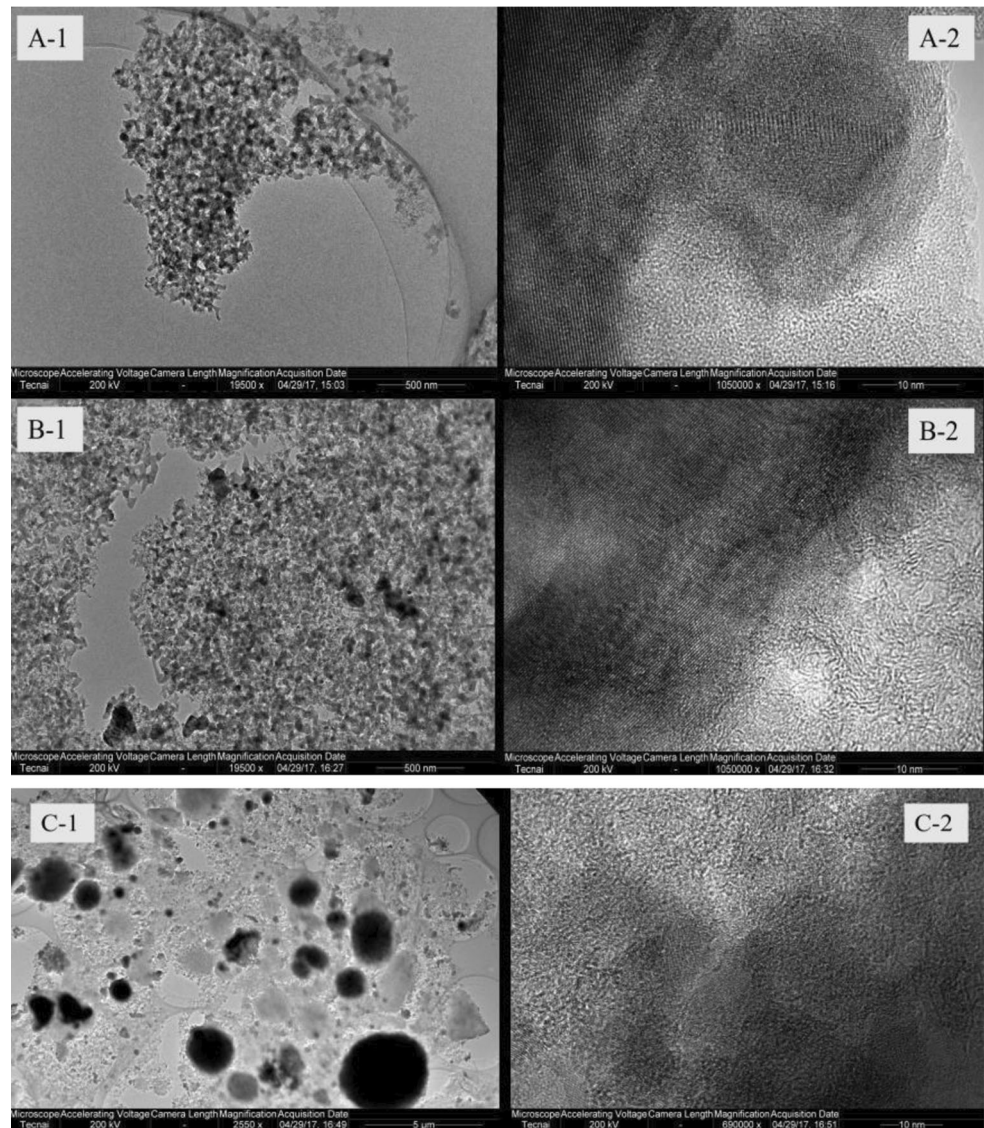
TEM images

The morphology of the magnetic mesoporous carbon composite is displayed by TEM images shown in Fig. 1. From the TEM images, it can be seen that the morphology of three kinds

Table 1 Synthetic conditions and performance

Sample number	m_{Fe} (g)	m_{CS} (g)	Calcined temperature (°C)
1	0.606	0.5	900
2	0.808	0.5	900
3	1.212	0.5	900
4	0.808	0.1	900
5	0.808	0.25	900

Fig. 1 TEM images of magnetic mesoporous carbon composite with 0.1 g chitosan (A-1 and A-2), 0.25 g chitosan (B-1 and B-2), and 0.5 g chitosan (C-1 and C-2) with different resolution ratios



of MMC are all amorphous and there are some black particles distributed in the carbon matrix formed by carbonization of chitosan. As the dosage of chitosan increases, the black particles turn into regular spherical shape and their particle sizes become larger, which is created due to thermal reduction reaction between carbon and iron, likely reducing ferric iron to zero-valent iron or Fe_3O_4 . Furthermore, as observed in the high-resolution TEM spectrogram, the regular stripes in black particles indicate that they are typical crystal structure.

XRD pattern

XRD is used for identifying the crystallographic structure of MMC with different chitosan contents. As shown in Fig. 2, the broad diffraction peaks between 20° and 25° appearing in all the XRD patterns are assigned to amorphous carbon (Li et al. 2017a; b), illustrating the formation of carbon skeleton through

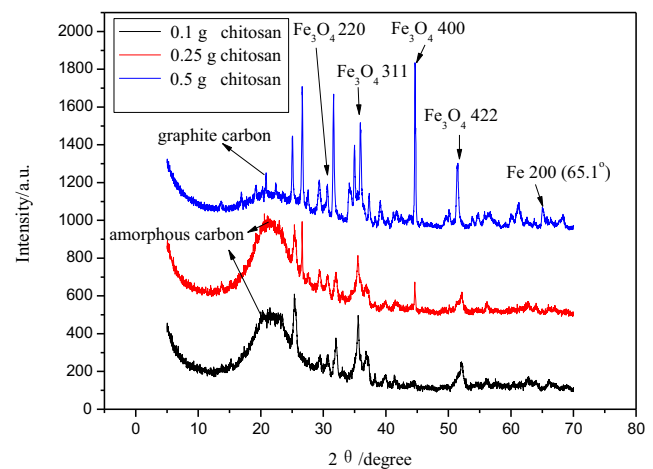


Fig. 2 XRD patterns of magnetic mesoporous carbon composites

calcination of the chitosan precursor and poor crystallinity of the carbon. The existence of four peaks at 30.7° , 35.6° , 44.5° , and 52° shown in the three spectrogram result matches well with pure Fe_3O_4 ((220), (311), (400), and (422), JCPDS, 85-1436) (Li et al. 2017a; b), which clearly demonstrates that Fe_3O_4 nanoparticles are successfully embedded in the carbon matrix. The peak at 65.1° is ascribed to the typical diffraction peak of Fe, which is indexed as (200) planes (Ma et al. 2017). Therefore, the results exhibit that the black particles found in the TEM images are the mixture of Fe_3O_4 and Fe.

FT-IR spectrum

Fourier transform infrared spectrometer, used to analyze the functional groups on the surface of the material, is one of the important means of characterization. The infrared spectrums of MMC with different chitosan contents are shown in Fig. 3. The peaks at 3400 , 3132 , and 3139 cm^{-1} represent the stretching vibration of $-\text{OH}$. The peaks at 2921 and 2857 cm^{-1} are contributed to the stretching vibration of $\text{C}-\text{H}$. There is a strong absorption peak at 1630 cm^{-1} , which ascribes to the stretching vibration of $\text{C}=\text{O}$. And the peak at 1397 cm^{-1} is index to the vibration of $\text{C}-\text{O}$. The sharp vibration bands at 1092 and 470 cm^{-1} are corresponding to $\text{Si}-\text{O}$. Besides, a set of weak peaks at 562 cm^{-1} in three MMC can be observed obviously, which is the typical peak of $\text{Fe}-\text{O}$. The above results reveal that the iron particles have already entered into the mesoporous carbon. In addition, there are plenty of functional groups such as $\text{O}-\text{H}$, $\text{C}-\text{O}$, and $\text{C}=\text{O}$ in the material.

BET analysis

The surface properties of three kinds of adsorbents are summarized in Table 1. According to the data, with the increase of the content of chitosan, the surface area and pore volume of

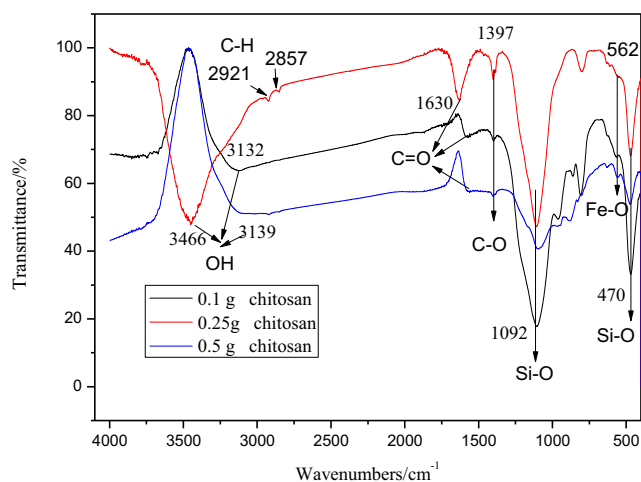


Fig. 3 IR spectra of magnetic mesoporous carbon composites

the material increase and the pore size decreases. These results demonstrate that with the increase of chitosan, a dense pore structure is formed, which leads to the decrease of the pore size and the increase of the specific surface area.

Effect of the content of Fe and chitosan on magnetism and adsorption performance

Based on the preparation method of MMC, it can be seen that the introducing of Fe into the mesoporous carbon contributes to the magnetism of composites. Besides, as carbon source, the content of chitosan will have tremendous influence on the adsorption capacity of the composites. Considering this, the effect of the content of Fe on magnetism of the prepared material and the effect of the content of chitosan on the adsorption performance are investigated and the results are showed in Fig. 4. As can be seen that, with the increasing of the content of Fe ranging from 0.606 g in sample 1, 0.808 g in sample 2, and 1.212 g in sample 3, the magnetism of MMC improves rapidly, which is in good agreement with our speculation. In addition, when the content of Fe is all set at 0.808 g (samples 2, 4, and 5) and the content of chitosan increases from 0.1 to 0.5 g , the higher content of chitosan in MMC results in the weaker magnetic properties of the material, which is possibly because the content of Fe per unit mass of MMC decreases. According to Fig. 4, another interesting result is the higher the content of chitosan is, the higher adsorption capacity of MO on MMC is (The content of chitosan in samples 1–3 is 0.5 g and is 0.1 and 0.25 g in samples 4 and 5, respectively). This reveals that the introduction of chitosan has a very significant influence on the adsorption capacity of MMC, which may be due to the abundance of functional groups provided by chitosan. Taking the above results, it can be concluded that the higher the content of Fe in MMC leads to the stronger the magnetism of MMC and the higher the content of chitosan contributes to the larger the adsorption capacity of MMC.

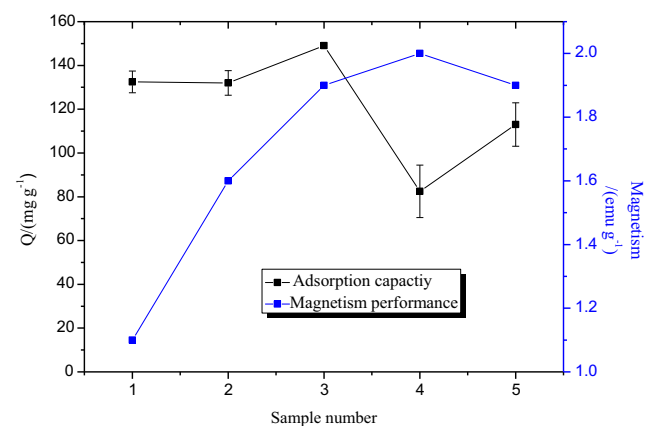


Fig. 4 The effect of the content of Fe and chitosan on magnetism and adsorption performance

Adsorption studies

Effect of pH

Solution pH is an important factor that affects both the chemical characteristic of template analytes and ionic state of functional groups on the surface of adsorbents. In this study, the effects of pH on the adsorption of MO by three materials during the pH value range of 2–7 are investigated, and the results are shown in Fig. 5. The adsorption of MO on the three prepared MMC increases as pH increased from 2 to 3. The adsorption capacity declines slightly at pH ranging from 3.0 to 4.0 and then no significant change in the adsorption can be observed with further changes in pH. Besides, the adsorption capacity of MO by the three MMCs enhances with the increasing of the content of chitosan, which may be due to the higher surface area and is in accordance with the measured data obtained from BET. Such phenomenon can be attributed to the ionic chemistry of the solution and surface charge of the adsorbents.

According to the Zeta potential analysis illustrated in Fig. 6, the isoelectric point of MMC (with 0.5 g chitosan) is 4.23. Therefore, it can be concluded that the potential of the surfaces of MMC are positive when $\text{pH} < 4.23$ and conversely negative when $\text{pH} > 4.23$. In the case of MO, it exists in an anionic sulfonate in the solution and carries a negative charge. Hence, during low pH values ($\text{pH} < 4.23$), the negatively charged MO (MO^-) can act with the protonated adsorbent (MMC^+) through electrostatic attraction, which contributes to the adsorption of MO. At the same time, large amounts of H^+ can compete with MMC^+ for MO^- , leading to a decrease in the binding of MMC^+ and MO^- . Furthermore, with increasing pH, the competition from H^+ becomes weaker, releasing more MO^- and producing higher adsorption of MO. And the number of positively charged sites on the surface of MMC

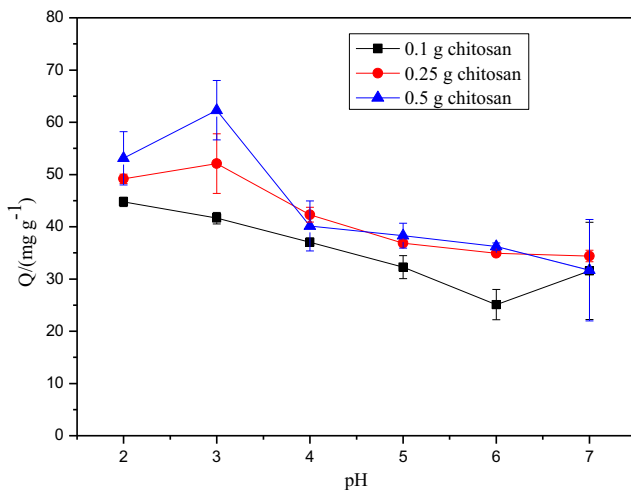


Fig. 5 The effect of pH value on the adsorption capacity of MO on magnetic mesoporous carbon composite

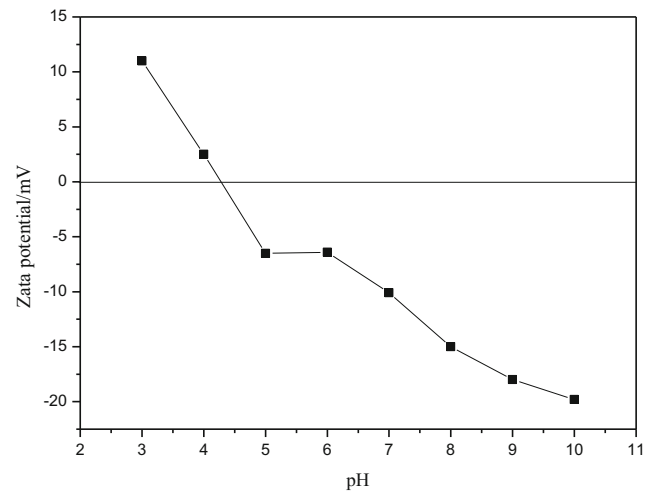


Fig. 6 Zeta potential of MMC with 0.5 g chitosan before adsorption

decreases with the increasing pH, which generates less adsorption of MO (Blaisi et al. 2018). At $\text{pH} > 4.23$, the interaction between adsorbent surfaces and anionic dyes is an electrostatic repulsive force, resulting in a lower adsorption of MO. Under this condition, the adsorption of MO may be due to the chemical interactions of carbonyl groups of composites with anions of dye molecules (Li et al. 2014). Because of the small solubility of MO, when the MO concentration is too high (100 mgL^{-1}), it tends to precipitate. Hence, pH 4 is selected in the subsequent experiments.

Effects of concentration and adsorption isotherm

The initial concentration of analytes is one of the most important factors affecting the adsorption capacity of the material. The effects of the initial concentration on the adsorption capacity of MO by MMC were studied. As the results in Fig. 7

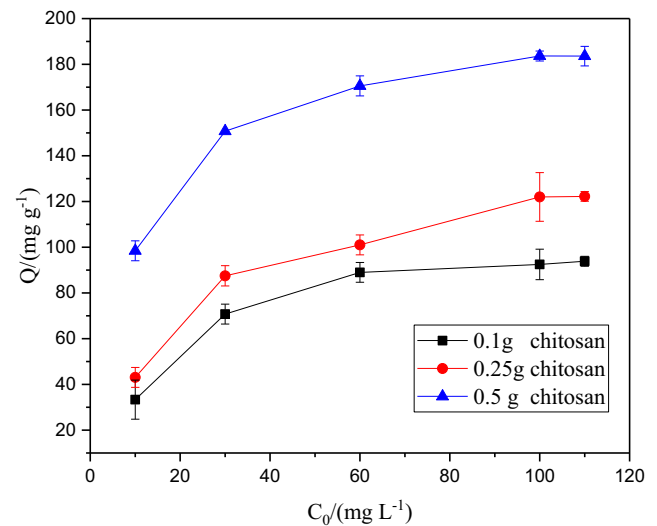


Fig. 7 The effect of initial MO concentration on the adsorption capacity of MO on magnetic mesoporous carbon composite

Table 2 BET analysis of magnetic mesoporous carbon composites

Chitosan content (g)	Specific surface ($\text{m}^2 \text{g}^{-1}$)	Pore volume ($\text{cm}^3 \text{g}^{-1}$)	Average pore diameter (nm)
0.1	136	0.84	24
0.25	169	0.91	20.8
0.5	244	0.61	10.1

show, along with the enhancing of the initial concentration of MO, the adsorption capacity of MO by MMC increases rapidly and then tends to be stable until the concentration reaches 110 mg L^{-1} . With the gradually increasing initial concentration of MO, the difference between the concentration of MO existing in the solution and the concentration of MO adsorbed on the surface of MMC increases, which generates the increase of mass transfer force and the diffusion rate of MO and leads to the higher adsorption capacity of MO by MMC. When the concentration of MO in the solution is high enough ($C = 100 \text{ mg L}^{-1}$), the active sites of the adsorbent will be fully occupied, which indicates that the MMCs attain saturation adsorption with the highest adsorption capacity. In addition, with the increase of the chitosan content, the adsorption capacity of MO on the three types of MMC increases greatly,

which might be due to the increasing specific surface area of the materials and much more functional adsorption groups of the adsorbents (Table 2).

Simultaneously, the effects of initial concentration on the adsorption capacity of MO by three MMC at different temperatures (298, 308, and 318 K) are also studied, and the results are shown in Fig. 8. For three MMC with different chitosan contents, the adsorption capacities are 94, 122, and 184 mg g^{-1} at 298 K, respectively, 119, 153, and 298 mg g^{-1} at 308 K, and 123, 191, and 389 mg g^{-1} at 318 K. From Fig. 7a, c, it can be concluded that in the case of MMC with different contents of chitosan, the adsorption capacity of MO by adsorbents increases with the increasing of temperature. Besides, under the same temperature, the adsorption capacity of MO by MMC enhances with the increase of the content of

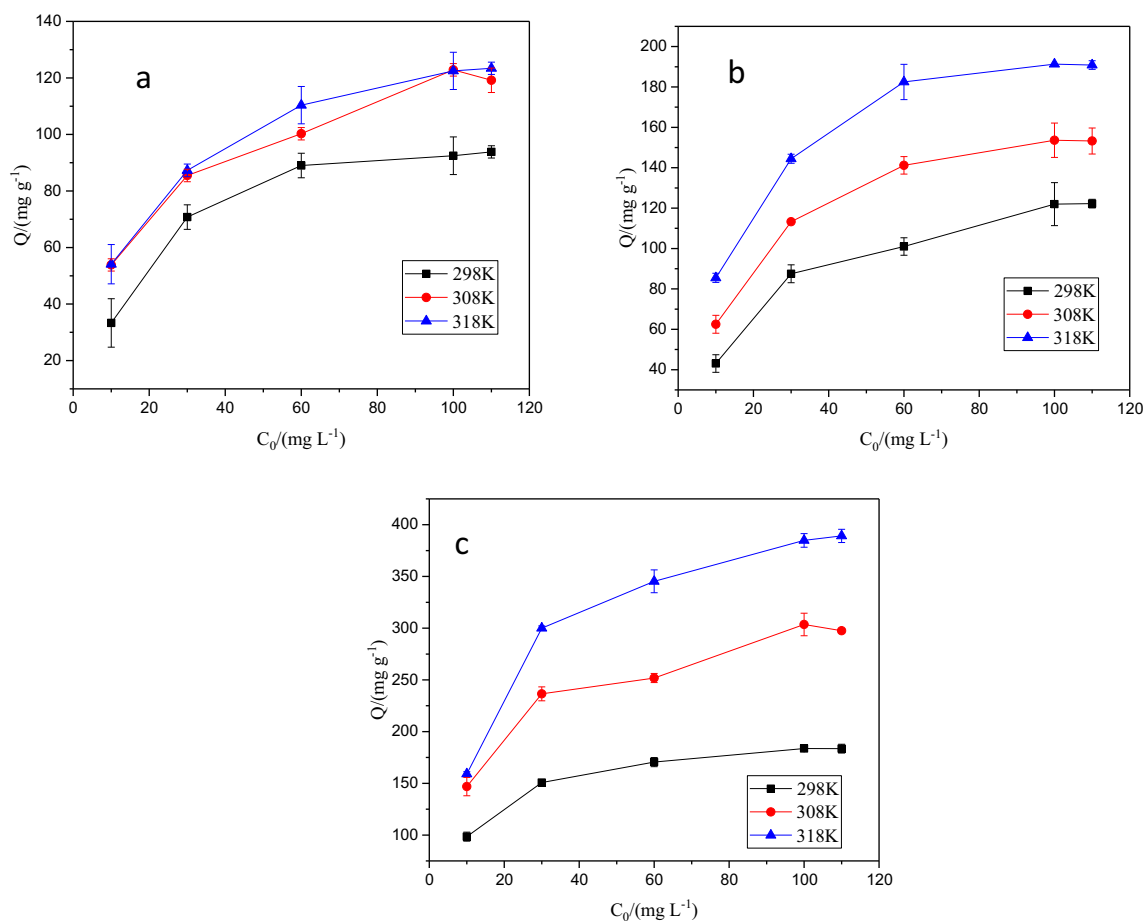


Fig. 8 The effect of initial MO concentration at different temperatures on the adsorption capacity of magnetic mesoporous carbon composite with 0.1 g chitosan (a), 0.25 g chitosan (b), and 0.5 g chitosan (c)

Table 3 Equilibrium parameters for the adsorption of MO onto MMC

Temperature (K)	MMC (0.1 g chitosan)			MMC (0.25 g chitosan)			MMC (0.5 g chitosan)		
	298	308	318	298	308	318	298	308	318
Langmuir									
q_m (mg g ⁻¹)	110.81	131.93	145.23	152.82	191.25	234.91	190.39	293.45	389.09
k_L (L mg ⁻¹)	0.0602	0.0808	0.0684	0.0375	0.0427	0.0582	0.1990	0.3346	0.2975
R^2	0.9840	0.9807	0.9774	0.9832	0.9971	0.9941	0.9892	0.9567	0.9715
ARE (%)	3.38	1.64	2.57	4.27	1.94	3.16	0.69	1.25	5.22
Freundlich									
n	3.08	3.41	3.16	2.43	2.53	2.87	5.19	5.28	4.77
K_F (mg g ⁻¹) (L mg ⁻¹) ^{1/n}	21.78	31.51	30.41	18.67	25.82	41.73	77.70	127.55	154.85
R^2	0.8963	0.9837	0.9931	0.9947	0.9822	0.9429	0.9608	0.9660	0.9644
ARE (%)	3.16	1.37	1.91	4.20	2.08	3.06	5.84	0.64	0.28

chitosan. These results reveal that temperature has a significant influence on the adsorption of MO by MMC, which will be evaluated in “[Thermodynamic study](#).”

The adsorption isotherm is an important method for determining the adsorption behavior of an adsorbent and understanding the adsorption mechanism. Therefore, Freundlich and Langmuir adsorption isotherms are adopted and compared to describe the adsorption process. The Langmuir and Freundlich models are expressed by the following equations, respectively:

$$q_e = \frac{q_m k_L C_e}{1 + (K_L C_e)} \tag{3}$$

$$q_e = k_F C_e^{1/nF} \tag{4}$$

where q_m (mg g⁻¹) is the maximum adsorption capacity, q_e (mg g⁻¹) is the equilibrium adsorption capacity, K_L (L mg⁻¹) is the equilibrium constant, and C_e (mg L⁻¹) is the equilibrium

concentration of MO. K_F is the Freundlich constant ((mg g⁻¹) (L mg⁻¹)^{1/n}) and 1/nF is the heterogeneity factor.

The isotherm parameters for the adsorption of MO onto MMC determined by Freundlich and Langmuir models are summarized in Table 3. As it can be observed, the R^2 of three materials in Langmuir isotherm are higher than those in Freundlich isotherm and average relative errors in Langmuir isotherm are all lower than 5.00%, indicating the Langmuir model is more suitable to represent the equilibrium data. Furthermore, the experimental data for the material containing 0.1 g chitosan (94, 119, and 130 mg g⁻¹) are close to calculated values (108, 136, and 139 mg g⁻¹). Similarly, the experimental data for the material containing 0.25 g chitosan (122, 153, and 191 mg g⁻¹) and 0.5 g chitosan (184, 298, and 389 mg g⁻¹) are both similar to calculated values. It can be seen that the adsorption of MO by three kinds of materials is consistent with the Langmuir equation, which

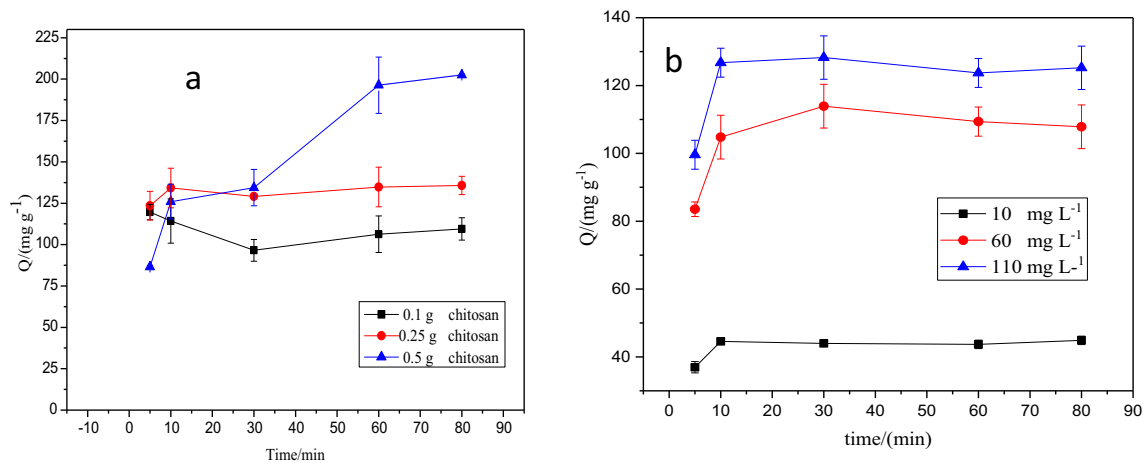


Fig. 9 The effect of contact time on the adsorption capacity of MO on magnetic mesoporous carbon composites with a different content (a) and the effect of contact time with a different initial concentration of MO on the adsorption capacity on magnetic mesoporous carbon composites with 0.25 g chitosan

Table 4 Parameters of the pseudo-first order and pseudo-second order for the adsorption of MO by MMC

	Concentration (mg L ⁻¹)	MMC (0.1 g chitosan)	MMC (0.25 g chitosan)			MMC (0.5 g chitosan)
			10	60	110	
Pseudo-first order						
q_1 (mg g ⁻¹)		108.87	44.18	109.04	125.74	291.84
k_1 (min ⁻¹)		0.0721	0.3619	0.2958	0.2141	0.3405
R^2		0.9758	0.9814	0.9908	0.9796	0.9540
ARE (%)		5.37	1.37	1.20	2.99	1.51
Pseudo-second order						
q_e (mg g ⁻¹)		118.87	45.18	124.27	127.00	299.75
k_2 (g (mg min) ⁻¹)		0.0012	0.0120	0.0036	0.0057	0.0026
R^2		0.9993	0.9822	0.9615	0.9992	0.9822
ARE (%)		5.01	1.47	1.18	3.01	1.52

illustrates that the binding sites of magnetic mesoporous carbon composite are on the surfaces equably and the adsorption of MO is regarded as uniform monolayer adsorption.

Effects of contact time and adsorption kinetics

Under the action of ultrasound, the MO molecule and the absorbents can be fully contacted, thus promoting the adsorption saturation of the material. The influence of the contact time on the adsorption of MO on three types of magnetic mesoporous materials is investigated, and the results are shown in Fig. 9a. It can be seen that the adsorption of MO on MMC with 0.1 g chitosan can obtain equilibrium instantaneously. When the content of chitosan increases to 0.25 g, the adsorption increases slightly in 10 min and then reaches the equilibrium. However, the adsorption of the material with 0.5 g chitosan increases violently in 60 min and at last becomes saturated. These results exhibited that with the increase of the amount of chitosan, the adsorption of MO on MMC needs more time to get equilibrium, which is because MMC with higher content of chitosan provides larger surface area and more functional groups. Furthermore, for the MMC containing

0.5 g chitosan, the adsorption of MO can be divided into two processes. In the first stage (10–60 min), owing to abundant MO, plentiful adsorption sites on the surface of MMC and huge mass transfer force of the system, the adsorption capacity increases rapidly. However, later on, with the decrease of adsorption sites on the surface of MMC, the adsorption rate slows down gradually until the adsorption equilibrium.

Simultaneously, the effect of contact time on the adsorption of MO by MMC with 0.25 g chitosan at different initial concentrations (10, 60, and 110 mg L⁻¹) are also evaluated. As the results in Fig. 9b show, the adsorption capacity enhances rapidly at the beginning and the adsorption equilibrium can be reached within only 10 min for 10, 60, and 110 mg L⁻¹ MO. And the adsorption capacity is 45, 108, and 125 mg g⁻¹ for 10, 60, and 110 mg L⁻¹, respectively, suggesting that with the increase of the initial concentration, the adsorption capacity also increases. This can be explained that the superior initial concentration can offer more reactants, which can fully act with the adsorption sites on the surface of the sorbent and promote the adsorption capacity effectively. Therefore, 60 min is selected as the best contact time in all subsequent experiments considering the efficiency of MO removal.

Table 5 Thermodynamic parameters for the adsorption of MO on MMC

Materials	T (K)	Q_e (mg g ⁻¹)	ΔG^0 (kJ mol ⁻¹)	ΔH^0 (kJ mol ⁻¹)	ΔS^0 (J mol ⁻¹ K ⁻¹)
MMC (0.1 g chitosan)	298	108	-11.15	16.39	92.87
	308	136	-12.40		
	318	139	-13.08		
MMC (0.25 g chitosan)	298	145	-12.12	25.58	126.62
	308	172	-13.45		
	318	208	-14.67		
MMC (0.5 g chitosan)	298	196	-13.25	33.14	156.12
	308	312	-15.06		
	318	400	-16.48		

The contact time is one of the important parameters for economical wastewater treatment application, and short equilibrium contact time can improve the efficiency of the application. The adsorption kinetics describes the solute uptake rate and in turn governs the equilibrium contact time of the sorption reaction. Hence, the kinetic data is used to fit the pseudo-first- and pseudo-second-order kinetic models, which is usually adopted to depict mass transfer processes, and the linear could be expressed as follows:

$$q_t = q_1(1 - \exp(-k_1 t)) \tag{5}$$

$$q_t = \frac{t}{(1/k_2 q_2^2) + (t/q_2)} \tag{6}$$

where k_1 (min^{-1}) and k_2 ($\text{g mg}^{-1} \text{min}^{-1}$) are the rate constants of the pseudo-first and pseudo-second-order models, respectively, q_1 and q_2 are the theoretical values for the adsorption capacity (mg g^{-1}), and t is the time (min).

Kinetic parameters obtained from pseudo-first- and pseudo-second-order models are displayed in Table 4. The high values of coefficient of determination and the low values of ARE indicated that the adsorption of MO by MMC was obeyed with the pseudo-second-order model and might be a rate-limiting step.

Thermodynamic study

In order to gain the information about the inherent energetic changes during the adsorption progress and get a better understanding of the adsorption mechanism, adsorption isotherms obtained at various temperatures are used to examine the thermodynamic study. The change in Gibbs free energies (G) are then calculated with Eq. (7) and ΔH^0 and ΔS^0 are calculated from Eq. (8):

$$\Delta G^0 = -RT \ln(\rho_w K_D) \tag{7}$$

$$\ln(\rho_w K_D) = \Delta S^0/R - \Delta H^0/RT \tag{8}$$

where R is the gas constant ($8.314 \text{ J mol}^{-1} \text{K}^{-1}$), T is the absolute temperature (K), K_D is the thermodynamic equilibrium constant (L mol^{-1}), and ρ_w is the water density (mg L^{-1}).

All the thermodynamic parameters are listed in Table 5. The negative values of ΔG^0 during all the temperature ranges reveal that the adsorption of MO by MMC is spontaneous and the decline in the value of ΔG^0 with increasing temperature demonstrates that the reaction is in favor of higher temperature. The positive value of ΔH^0 illuminates that the adsorption process is endothermic; therefore, a higher adsorption capacity can be obtained at higher temperature. Furthermore, the positive values of ΔS^0 mean the randomness increased at the solid-solution interface, which is mostly because of the interaction between MO and MMC.

Desorption and regeneration

The practical application of an adsorbent in the remediation treatment rests on the adsorption capacity and reusability of adsorbent. So, in order to check the economic feasibility of the adsorption process, desorption experiments and reusability experiments are performed in this study. From Fig. 4, it can be observed that the adsorption capacity of MO by MMC during the alkaline medium is very low, implying alkaline medium is harmful for the adsorption and alkali treatment is a feasible approach to regenerating. According to the above consideration, 0.1 M NaOH is used to desorb MO from MMC and the results show that desorption efficiency can be high to 90%. Besides, the results of adsorption–desorption cycles reveal that the adsorption of MO by MMC nearly maintain unchanged after five operation cycles, illustrating MMC is an efficient and economical adsorbent.

Conclusions

In this work, magnetic mesoporous carbon materials with a large surface area of $244 \text{ m}^2 \text{g}^{-1}$ and high adsorption performance were successfully synthesized for the removal of MO. TEM results showed that the spherical particles had distributed into the graphited carbon matrix. According to IR results, it could be seen that the prepared materials were rich in hydroxyl and carbonyl groups, which could react with MO effectively. Besides, the study of the effect of the content of Fe and the content of chitosan in MMC on the magnetism and adsorption performance of prepared material indicated that the content of Fe is proportional to the magnetic properties of MMC and the high content of chitosan contributes to high adsorption capacity of MMC. In addition, the effects of pH value, initial concentration of methyl orange, and contact time on the adsorption performance of MO were evaluated, respectively. At 318 K, when the content of chitosan in MMC increased from 0.1 to 0.5 g, the maximum adsorption capacity of MO on MMC increased from 139 to 400 mg g^{-1} . Kinetic studies demonstrated that the adsorption process obeyed a pseudo-second-order kinetic model, which indicated that the adsorption process is controlled by the rate-limiting step. At last, the generation experiments revealed that the saturated materials could be desorbed by 0.1 mol L^{-1} NaOH efficiently and reused five times at least. These results illustrated MMC was an efficient and economical adsorbent for the adsorption of MO.

Funding information This work was supported by National Natural Science Foundation of China (21607075) and Fundamental Research Funds for the Central Universities (KJQN201721 and KYZ201600163).

References

- Blaisi NI, Zubair M, Ihsanullah AS, Kazeem TS, Manzar MS, Al-Kutti W, Harthi AMA (2018) Date palm ash-MgAl-layered double hydroxide composite: sustainable adsorbent for effective removal of methyl orange and eriochrome black-T from aqueous phase. *Environ Sci Pollut Res* 25(34):34319–34331. <https://doi.org/10.1007/s11356-018-3367-2>
- Cadaval TRS, Dotto GL, Pinto LAA (2015) Equilibrium isotherms, thermodynamics, and kinetic studies for the adsorption of food Azo dyes onto chitosan films. *Chem. Eng. Commun.* 202:1316–1323. <https://doi.org/10.1080/00986445.2014.934449>
- Coromelci-Pastravanu C, Ignat M, Popovici E, Harabagiu V (2014) TiO₂-coated mesoporous carbon: conventional vs. microwave-annealing process. *J Hazard Mater* 278:382–390. <https://doi.org/10.1016/j.jhazmat.2014.06.036>
- Dai H, Peng X, Yang W, Hu F, Qiu Z, Zou Y (2018) Synthesis and characterization of graphitic magnetic mesoporous nanocomposite and its application in dye adsorption. *J Mol Liq* 253:197–204. <https://doi.org/10.1016/j.molliq.2018.01.030>
- Deng Y, Cai Y, Sun Z, Zhao D (2011) Magnetically responsive ordered mesoporous materials: a burgeoning family of functional composite nanomaterials. *Chem Phys Lett* 510:1–13. <https://doi.org/10.1016/j.cplett.2011.04.093>
- Deng J, Chen Y, Lu Y, Ma X, Feng S, Gao N, Li J (2017) Synthesis of magnetic CoFe₂O₄/ordered mesoporous carbon nanocomposites and application in Fenton-like oxidation of rhodamine B. *Environ Sci Pollut Res* 24:14396–14408. <https://doi.org/10.1007/s11356-017-8941-5>
- Fuertes AB, Sevilla M, Valdes-Solis T, Tartaj P (2007) TiO₂-coated mesoporous carbon: conventional vs. microwave-annealing process. *Chem Mater* 19:5418–5423. <https://doi.org/10.1021/cm071713k>
- Ghugre SP, Saroha AK (2018) Catalytic ozonation for the treatment of synthetic and industrial effluents—application of mesoporous materials: a review. *J Environ Manag* 27:1042–1056. <https://doi.org/10.1016/j.jenvman.2018.01.052>
- Hao G, Li W, Wang S, Zhang S, Lu A (2010) Tubular structured ordered mesoporous carbon as an efficient sorbent for the removal of dyes from aqueous solutions. *Carbon* 48:3330–3339. <https://doi.org/10.1016/j.carbon.2010.05.011>
- Holec D, Kostoglou N, Tampaxi C, Babic B, Mitterer C, Rebholz C (2018) Theory-guided metal-decoration of nanoporous carbon for hydrogen storage applications. *Sur Coat Tech* 351:42–49. <https://doi.org/10.1016/j.surfcoat.2018.07.025>
- Li J, Shao Z, Chen C, Wang X (2014) Hierarchical GOs/Fe₃O₄/PANI magnetic composites as adsorbent for ionic dye pollution treatment. *RSC Adv* 4:38192–38198. <https://doi.org/10.1039/c4ra05800c>
- Li Z, Huang Y, Yuan L, Hao Z, Huang Y (2015) Status and prospects in sulfur-carbon composites as cathode materials for rechargeable lithium-sulfur batteries. *Carbon* 92:41–63. <https://doi.org/10.1016/j.carbon.2015.03.008>
- Li M, Jiao C, Yang X, Wang C, Wu Q, Wang Z (2017a) Magnetic N-doped mesoporous carbon as an adsorbent for the magnetic solid-phase extraction of phthalate esters from soft drinks. *J Sep Sci* 40:1637–1643. <https://doi.org/10.1002/jssc.201601262>
- Li S, Liu L, Yu Y, Wang G, Zhang H, Chen A (2017b) Fe₃O₄ modified mesoporous carbon nanospheres: magnetically separable adsorbent for hexavalent chromium. *J Alloy Compd* 698:20–26. <https://doi.org/10.1016/j.jallcom.2016.12.163>
- Liang T, Wang F, Liang L, Liu M, Sun J (2016) Magnetically separable nitrogen-doped mesoporous carbon with high adsorption capacity. *J Mater Sci* 51:3868–3879. <https://doi.org/10.1007/s10853-015-9706-5>
- Libbrecht W, Verberckmoes A, Thybaut JW, Voort VDP, De Clercq J (2017) Soft templated mesoporous carbons: tuning the porosity for the adsorption of large organic pollutants. *Carbon* 116:528–546. <https://doi.org/10.1016/j.carbon.2017.02.016>
- Liu Z, Fu D, Liu F, Han G, Liu C, Chang Y, Xiao Y, Li M, Li S (2014) Mesoporous carbon nanofibers with large cage-like pores activated by tin dioxide and their use in supercapacitor and catalyst support. *Carbon* 70:295–307. <https://doi.org/10.1016/j.carbon.2014.01.011>
- Liu M, Deng X, Zhu D, Duan H, Xiong W, Xu Z, Gan L (2016) Magnetically separated and N, S co-doped mesoporous carbon microspheres for the removal of mercury ions. *Chinese Chem Lett* 27:795–800. <https://doi.org/10.1016/j.ccllet.2016.01.038>
- Liu S, Lei W, Liu Y (2019) Rational design of few-layered ReS₂ nanosheets/N-doped mesoporous carbon nanocomposites for high-performance pseudocapacitive lithium storage. *Chem Eng J* 356:1052–1061. <https://doi.org/10.1016/j.cej.2018.09.132>
- Ma C, Gao Q, Zhou J, Chen Q, Han B, Xia K, Zhou C (2017) Facile one-pot synthesis of magnetic nitrogendoped porous carbon for high-performance bilirubin removal from BSA-rich solution. *RSC Adv* 7:2081–2091. <https://doi.org/10.1039/c6ra25027k>
- Quiroa-Montalván CM, Gómez-Pineda LE, Álvarez-Contreras L, Valdez R, Arjona N, Oropeza-Guzmán MT (2017) Ordered mesoporous carbon decorated with magnetite for the detection of heavy metals by square wave anodic stripping voltammetry. *J Electrochem Soc* 164(6):B304–B313. <https://doi.org/10.1149/2.0231707jes>
- Rodrigues DAS, Moura JM, Dotto GL, Cadaval TRS Jr, LAA P (2018) Preparation, characterization and dye adsorption/reuse of chitosanvanadate films. *J. Polym. Environ.* 26:2917–2924. <https://doi.org/10.1007/s10924-017-1171-6>
- Su Y, Li S, Wu D, Zhang F, Liang H, Gao P, Cheng C, Feng X (2012) Two-dimensional carbon-coated graphene/metal oxide hybrids for enhanced lithium storage. *ACS Nano* 6(9):8349–8356. <https://doi.org/10.1021/nn303091t>
- Suib SL (2017) A review of recent developments of mesoporous materials. *Chem Rec* 17:1169–1183. <https://doi.org/10.1002/tcr.201700025>
- Tang L, Yang G, Zeng G, Cai Y, Li S, Zhou Y, Pang Y, Liu Y, Zhang Y, Lun B (2014) Synergistic effect of iron doped ordered mesoporous carbon on adsorption-coupled reduction of hexavalent chromium and the relative mechanism study. *Chem Eng J* 239:114–122. <https://doi.org/10.1016/j.cej.2013.10.104>
- Tripathi PK, Gan LH, Liu MX, Rao NN (2014) Mesoporous carbon nanomaterials as environmental adsorbents. *J Nanosci Nanotechnol* 14(2):1823–1837. <https://doi.org/10.1166/jnn.2014.8763>
- Walcarius A (2017) Recent trends on electrochemical sensors based on ordered mesoporous carbon. *Sensors* 17:1863–1905. <https://doi.org/10.3390/s17081863>
- Wang J, Liu H, Sun H, Hua W, Wang H, Liu X, Wei B (2018) One-pot synthesis of nitrogen-doped ordered mesoporous carbon spheres for high-rate and long-cycle life supercapacitors. *Carbon* 127:85–92. <https://doi.org/10.1016/j.carbon.2017.10.084>
- Wu Z, Li W, Webley PA, Zhao D (2012) General and controllable synthesis of novel mesoporous magnetic iron oxide@carbon encapsulates for efficient arsenic removal. *Adv Mater* 24:485–491. <https://doi.org/10.1002/adma.201103789>
- Yadaei H, Beyki MH, Shemirani F, Nouroozi S (2018) Ferrofluid mediated chitosan@mesoporous carbon nanohybrid for green adsorption/preconcentration of toxic Cd(II): modeling, kinetic and isotherm study. *React Funct Polym* 122:85–97. <https://doi.org/10.1016/j.reactfunctpolym.2017.10.011>

- Zeng G, Liu Y, Tang L, Yang G, Pang Y, Zhang Y, Zhou Y, Li Z, Li M, Lai M, He X, He Y (2015) Enhancement of Cd(II) adsorption by polyacrylic acid modified magnetic mesoporous carbon. *Chem Eng J* 259:153–160 <https://doi.org/10.1016/j.cej.2014.07.115>
- Zhai Y, Dou Y, Liu X, Tu B, Zhao D (2009) One-pot synthesis of magnetically separable ordered mesoporous carbon. *J Mater Chem* 19: 3292–3300. <https://doi.org/10.1039/b821945a>
- Zhang LF, Hu ZP, Gao ZM, Liu YL, Yuan ZY (2015) Preparation and catalytic application of ordered mesoporous carbon-based metal composite materials. *Prog Chem* 27(8):1042–1056. <https://doi.org/10.7536/PC150318>
- Zhang P, Zhang J, Dai S (2016) Mesoporous carbon materials with functional compositions. *Chem Eur J* 23(201):1986–1998. <https://doi.org/10.1002/chem.201602199>

Publisher's note Springer Nature remains neutral with regard to jurisdictional claims in published maps and institutional affiliations.